

# Modal Parameter Estimation from Operating Data

Mark Richardson & Brian Schwarz

Vibrant Technology, Inc.

Jamestown, California

Modal testing, also referred to as Experimental Modal Analysis (EMA), underwent a revolutionary change during the early 1970's with the implementation of the Fast Fourier Transform (FFT) in computer-based FFT analyzers. Prior to that time, model testing had been done primarily with analog equipment. FFT-based EMA, on the other hand, required the development of new digital signal processing methods.

Modal parameter estimation is a key step in FFT-based EMA. This one step, also called curve fitting, has probably received more attention than any other during the past 30 years. Numerous methods have been developed, and the technical literature contains 100's of papers documenting many different approaches.

Modal analysis is used to characterize resonant vibration in machinery and structures. A mode of vibration is defined by three parameters; modal frequency, a modal damping value and a mode shape. Modal parameter estimation is the process of determining these parameters from experimental data. It can also be shown that a set of modal parameters *completely characterizes* the dynamic properties of a structure. This set of parameters is also called a modal model for the structure.

Two recent S&V articles have described different approaches to modal testing; one that relies on carefully controlled multi-shaker excitation [3], and the other that strongly suggests that artificial excitation is not required at all [4]. Regardless of whether artificial excitation is used or not, both approaches rely heavily on modal parameter estimation. Both articles devote the majority of their discussion to this subject.

## How Much Accuracy Is Required?

Although time, budget, and physical constraints will most certainly play a part, the modal testing method you choose will strongly depend on what you intend to do with the modal data. The two most common uses of modal data are,

1. Trouble shooting noise or vibration problems.
2. Confirming the validity of computer generated finite element models.

Finite element analysis (FEA) is commonly used today in the development of most new machines, structures, and products of all kinds. Once a finite element model is validated, it can be used for simulations, calculating stresses and strains, and for investigating the effects of structural modifications on its vibration properties. Since both EMA and

FEA yield a set of modes for a structure, modal parameters are used to compare experimental and analytical results.

Trouble shooting only requires enough data to characterize the problem so that a solution can be found. Verifying a finite element model usually requires much more extensive and accurate modal testing.

If no artificial excitation is required and excitation forces don't have to be measured, simply acquiring and processing operating response data sounds like an easier way to do modal testing. When possible however, controlling and measuring the excitation forces is the preferred way to do modal testing because the assumptions required for modal parameter estimation are less restrictive. But for those cases where the excitation forces are not known and/or cannot be measured, curve fitting a set of measurements post-processed from operating data can still provide usable modal parameter estimates.

## What Is Operating Data?

Operating data is certainly what the name implies. It is data that is acquired while a machine or structure is undergoing vibratory motion during its operation or use. For modal parameter estimation, the definition can be extended further.

*Operating Data is any vibration data that is acquired without simultaneously acquiring the excitation forces.*

## Shape Data

Whenever the vibration responses at two or more points and directions (degrees-of-freedom or DOFs) on the surface of a structure are measured, a vibration *shape* is defined. That is, a shape defines the magnitude and phase of the motion of one DOF relative to any other DOF.

*An Operating Deflection Shape (ODS) is the magnitudes and phases of two or more DOFs of operating data acquired from a machine or structure.*

An ODS, therefore, defines the *relative motion* between two or more DOFs on a structure. An ODS can be defined for a specific frequency or for a moment in time [2].

Structural resonances can be thought of as *structural weaknesses*. That is, are certain *natural* frequencies, a structure will readily absorb energy and vibrate with an *excessive level of vibration*. Therefore, as the frequency of a (single frequency) sinusoidal excitation force approaches one of its resonant frequencies, the vibration level of a structure will grow.

When sinusoidal excitation is applied to a structure at or near a modal frequency, its sinusoidal response or deformation will be *dominated* by its resonant vibration. Furthermore, its ODS will *look like* the mode shape associated with the resonance.

### Observing Mode Shapes

One of the earliest modal testing methods takes advantage of this property of structures, allowing one to actually *see* its mode shapes. Strobe light testing was used to observe mode shapes long before digital computers or FFT analyzers were available.

A strobe light test is very straightforward. While exciting a structure with a shaker driven by a sine wave signal, the structure surface is illuminated with a strobe light that is triggered by the sine wave signal. This causes the deformation of the surface to *stand still*, displaying the ODS of the structure at that frequency. If the excitation frequency is then adjusted to be close to a modal frequency, the ODS becomes *dominated* by the mode shape, and hence is a close approximation of the mode shape.

Using a strobe light is still probably the cheapest and easiest way to do modal testing today. It does, however, have some drawbacks. In general, it works best on smaller structures and in darkness, and it requires that the deformation of the structure be visible. Also, there is no preservation of the data for further post analysis.

A modern implementation of this technique uses a laser vibrometer to rapidly scan the surface of the structure, measuring the surface velocity at many points, and displaying the ODS using a color map on a computer screen. The cost of this equipment is of course much higher than a strobe light, but at least the ODS data can be saved for further use.

Both of these modal testing techniques are measuring operating data in the sense that the sinusoidal excitation force is not measured. Although both techniques employ a carefully controlled excitation force, they both suffer in several ways compared to other techniques,

1. Since only one mode is excited at a time, some type of search procedure must be used to locate all of the modes. This can be time consuming.
2. Exciting just one mode and not several at a time can be difficult, if not impossible, with many structures.
3. Only the modal frequency and mode shape are estimated. Modal damping is not estimated.

### Broad Band Excitation

All excitation forces can be classified as either *narrow band* like a single frequency sine wave, or *broad band*. The most common broad band signals are random, swept sine or chirp, and transient or impulsive [5]. Variations of these signals include burst random, burst chirp, and random transient.

A sine wave is classified as narrow band because its spectrum is very narrow, containing essentially a single non-zero frequency. All of the broad band signals have a non-zero frequency spectrum over a broad range of frequencies.

Broad band excitation signals have the following advantages,

1. They excite many modes at a time.
2. They can be controlled to minimize distortion or non-linear response of the structure. (Modes are only defined for structures that obey a set of linear, stationary equations of motion.)
3. They can be designed to minimize a signal processing error caused by the FFT called *leakage*.
4. Random signals can be used together with spectrum ensemble averaging to effectively *linearize* the non-linear response of a structure.
5. Many structures are excited by ambient forces which can be assumed to be broad band in nature.

### Structural Dynamic Models

All modal testing is based on the assumption that the vibrational behavior of a mechanical structure can be represented either by a set of differential equations in the time domain, or by a set of algebraic (spectral) equations in the frequency domain.

#### Time Domain Model

Modes are defined as *solutions* to the time domain differential equations shown in Figure 1.

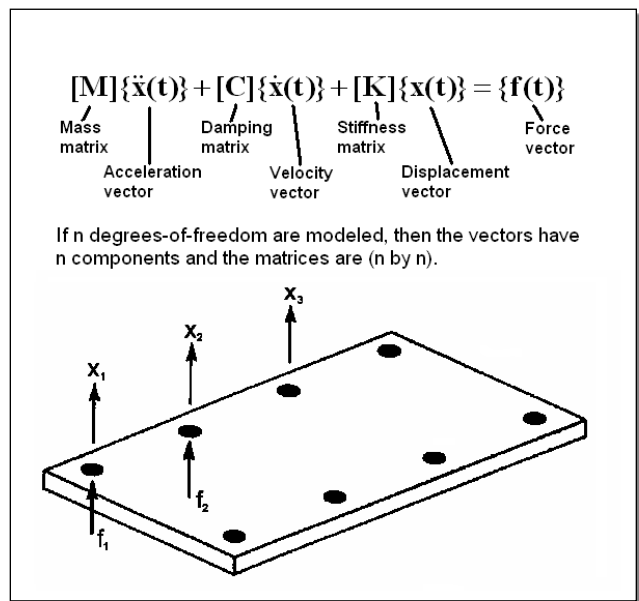


Figure 1. Time Domain Dynamic Model.

This set of time domain differential equations describes the dynamics between n-discrete DOFs of the structure. Equations are defined between as many DOFs on a structure as

necessary to adequately describe its dynamic behavior.

For real structures, these equations are usually defined by using finite element modeling to derive the mass and stiffness matrices. (Damping is ignored because it is too difficult to model.) From an experimental point of view however, it is more straightforward to define the equations of motion in the frequency domain.

### Frequency Domain Model

The dynamic behavior between any pair of DOFs of a machine or structure is described in the frequency domain by a transfer function. A transfer function matrix model describes the dynamics between n-DOFs of the structure, and contains transfer functions between all combinations of DOF pairs, as shown in Figure 2.

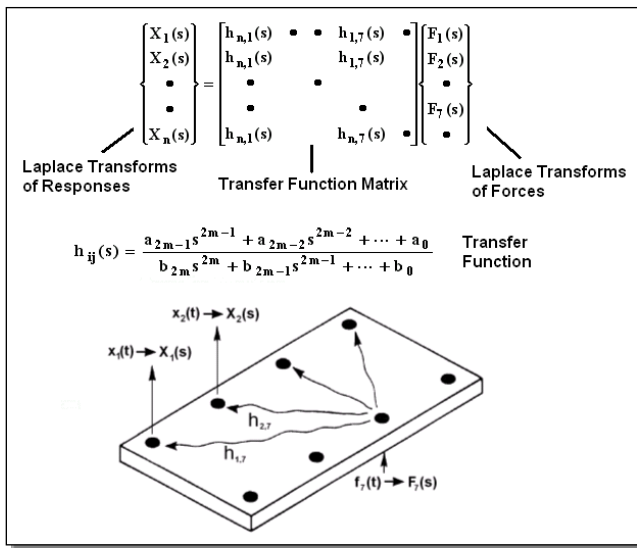


Figure 2. Frequency Domain Dynamic Model.

Even though these equations don't explicitly contain mass, damping, or stiffness matrices, nevertheless all of the inertial (mass), elastic (stiffness) and energy dissipating (damping) properties of a real structure are contained in the transfer functions.

### Frequency Response Function (FRF)

Figure 3 contains a plot on the S-plane of a transfer function for a single mode or resonance. Notice that it is only plotted over half of the S-plane so that its values along the  $j\omega$ -axis can be clearly seen. Since the Laplace variable is complex valued, the transfer function is also complex valued. Therefore, it is plotted both as real and imaginary parts and as magnitude and phase. The S-plane is also called the complex frequency domain.

Any element of the transfer function matrix can be measured from a real structure. However, instead of measuring it over the entire S-plane, only its values along the  $j\omega$ -axis are actually measured.

*The transfer function evaluated along the  $j\omega$ -axis in the S-plane is called the Frequency Response Function (FRF).*

Figure 3 shows the FRF for a single resonance plotted along the  $j\omega$ -axis.

All commercially available FFT analyzers are capable of estimating an FRF in the presence of extraneous measurement noise. This involves *simultaneously acquiring* both an excitation force signal and a corresponding vibration response signal, followed by some digital signal processing [5].

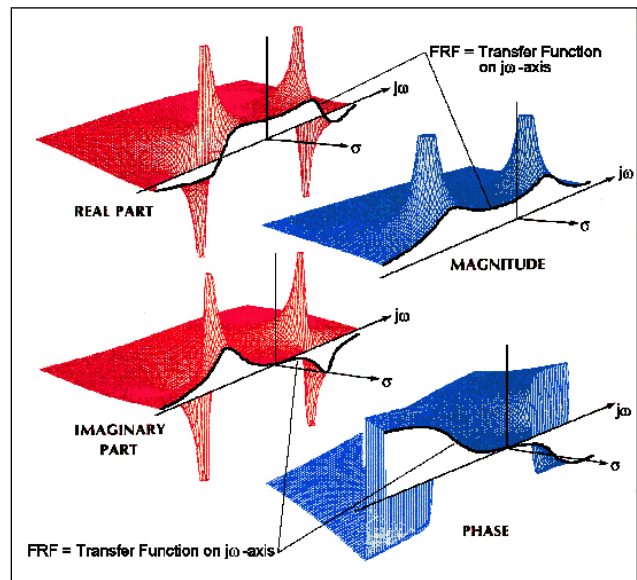


Figure 3. Transfer Function and FRF for a Single Mode.

### Modal Frequency and Damping

Notice that the transfer function in Figure 3 has two peaks in it, and that its value goes to *infinity* at the peaks. The locations of these peaks are called the *poles* of the transfer function.

*The coordinates of a pole are the modal frequency and damping of a mode.*

Several well known definitions of modal frequency and damping are shown in Figure 4.  $\sigma_0$  is called the *half power point* damping, and will be used for curve fitting comparisons later on.



$\mathbf{t}$  – denotes the transposed vector.

The following assumptions were made in order to derive equation (5).

1. **Linearity:** The structural dynamics are linear and stationary, and are adequately described by either the time domain (1) or frequency domain (2) equations.
2. **Maxwell's Reciprocity:** The matrices in either the time domain or frequency domain equations are symmetric.
3. **Distinct Pole Locations:** Each resonance is described by a pair of distinct poles.

### Measuring One Row or Column of FRFs

Since the mode shape is contained in every row and column, of the residue matrix,

*Only one row or column of the FRF matrix needs to be measured and curve fit in order to obtain mode shapes.*

Another way of putting equation (4) into words is,

*Every row and column of the residue matrix contains the mode shape multiplied by one of its own components.*

This makes it clear that if a row or column is chosen where the mode shape is zero, called a *nodal point*, then the entire row or column of residues for that mode will be zero also. This conclusion, of course, is known by every modal testing practitioner. In other words, if the structure is excited or its response is measured at the nodal point of a mode shape, no FRF measurements from the row or column will contain a resonance peak for that mode.

### Impulse Response Function

Since the IRF is the Inverse Fourier transform of the FRF, each element of an FRF matrix has an equivalent IRF in the time domain. Modal parameters are therefore estimated from *one row or column* of an IRF matrix in the same way as they are estimated from one row or column of an FRF matrix.

### Time Domain Curve Fitting Model

An IRF matrix with the same size and DOFs as its corresponding FRF matrix is represented as a summation of exponential terms with modal parameters in them,

$$[\mathbf{I}(t)] = \sum_{k=1}^m \left( [\mathbf{r}_k] e^{\mathbf{p}_k(t)} + [\mathbf{r}_k^*] e^{\mathbf{p}_k^*(t)} \right) \quad (6)$$

where:

$$[\mathbf{I}(t)] = (n \text{ by } n) \text{ IRF matrix.}$$

Note that just like the FRFs, each IRF is also a summation of contributions due to each mode, and that each modal contribution is itself a summation of two *complex exponential* terms.

Equation (6) can be rewritten as a summation of damped sinusoidal responses, making it clear that it is indeed the analytical expression for an IRF, as shown in Figure 5.

$$[\mathbf{I}(t)] = \sum_{k=1}^m \left[ |\mathbf{r}_k| e^{-\sigma_k(t)} \sin(\omega_k t + \alpha_k) \right] \quad (7)$$

where:

$|\mathbf{r}_k| = (n \text{ by } n) \text{ matrix of residue magnitudes.}$

$\alpha_k = (n \text{ by } n) \text{ matrix of residue phases.}$

Expression (7) clearly shows the role that each modal parameter plays in an IRF. Modal damping ( $\sigma_k$ ) defines the exponential decay envelope for each mode, modal frequency ( $\omega_k$ ) defines the sinusoidal frequency for each mode, and the residue defines the amplitude of response of each mode.

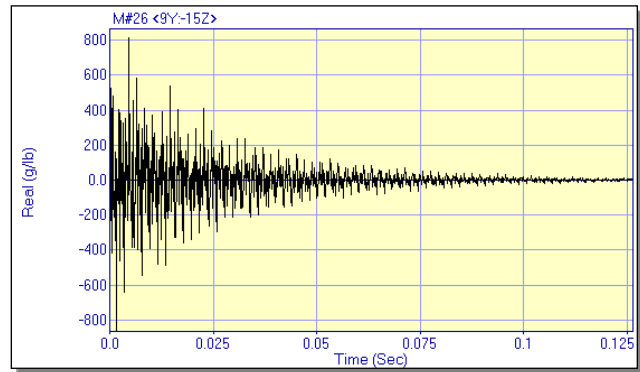


**Figure 5. An IRF.**

The Complex Exponential curve fitting method uses the analytical model (6) to estimate the modal parameters of a structure from experimental IRF data.

### Response Spectrum Matrix

The subject of this article is estimating modal parameters from operating data. Recall that operating data is acquired in any situation where the excitation forces are not measured.

Is it possible to curve fit operating data using an FRF or IRF curve fitting model? The answer is “Yes”, but a strong assumption regarding the unknown excitation forces is required.

An FRF matrix model is obtained by substituting  $\mathbf{s} = \mathbf{j}\omega$  into the transfer matrix model in Figure 2,

$$\{\mathbf{X}(\mathbf{j}\omega)\} = [\mathbf{H}(\mathbf{j}\omega)]\{\mathbf{F}(\mathbf{j}\omega)\} \quad (8)$$

where:

$\{\mathbf{X}(\mathbf{j}\omega)\} = n\text{-dimensional vector of response Fourier transforms.}$

$\{\mathbf{F}(\mathbf{j}\omega)\} = n\text{-dimensional vector of force Fourier transforms.}$

$[\mathbf{H}(\mathbf{j}\omega)] = (\mathbf{n} \text{ by } \mathbf{n})$  FRF matrix.

The Response Spectrum matrix is formed by taking the *outer product* of equation (8) with itself.

$$[\mathbf{G}_{\mathbf{x},\mathbf{x}}(\mathbf{j}\omega)] = [\mathbf{H}(\mathbf{j}\omega)][\mathbf{G}_{\mathbf{r},\mathbf{f}}(\mathbf{j}\omega)][\mathbf{H}(\mathbf{j}\omega)]^T \quad (9)$$

where:

$[\mathbf{G}_{\mathbf{x},\mathbf{x}}(\mathbf{j}\omega)] = \{\mathbf{X}(\mathbf{j}\omega)\}\{\mathbf{X}(\mathbf{j}\omega)\}^T = (\mathbf{n} \text{ by } \mathbf{n})$  Response Spectrum matrix.

$[\mathbf{G}_{\mathbf{r},\mathbf{f}}(\mathbf{j}\omega)] = \{\mathbf{F}(\mathbf{j}\omega)\}\{\mathbf{F}(\mathbf{j}\omega)\}^T = (\mathbf{n} \text{ by } \mathbf{n})$  Force Spectrum matrix.

$\mathbf{T}$  – denotes the transposed complex conjugate.

Each row or column of the Response Spectrum matrix contains the spectrum of each measured response multiplied by the conjugate spectrum of a reference (or fixed) response. Each row or column corresponds to a different reference response. The diagonal elements of the Response and Force Spectrum matrices above are called *Auto Spectra*, and the non-diagonal elements are called *Cross Spectra*.

A row or column of the Response Spectrum matrix can be curve fit to estimate modal parameters, provided that the following assumption is made.

**Flat Force Spectrum:** *If the excitation Force Spectrum matrix can be assumed to be “relatively flat” over in the frequency range of the modes of interest, then elements of the Response Spectrum matrix can be curve fit using an FRF (or IRF) curve fitting model.*

If the excitation forces are known to have a flat spectrum over the frequency range of the modes of interest, then the peaks in a Response Spectrum are caused by structural resonances. But the difficulty with all operating data is that unless the forces can be measured, there is no guarantee that the above assumption is met.

If a machine or structure contains any rotating or reciprocating parts, its Force Spectrum matrix will not be flat. Even in cases where a structure is excited using a flat force spectrum, impedance mismatches between the exciter and the structure will cause peaks in the response spectrum that are not due to resonances. Impedance mismatches can also cause the Force Spectrum to dip at resonance peaks.

On the other hand, there are excitation forces that can be assumed to have a flat spectrum. For instance, traffic on a bridge or wind blowing against a building are assumed to be broad-band and random in nature, with a flat spectrum. If an excitation force is impulsive in nature, its spectrum is also assumed to be flat.

## The Response Spectrum and the FRF

To see more clearly how an FRF curve fitting model is applied to a row or column of Response Spectrum matrix data, consider a case of only one (unknown) excitation force. Using equation (8), the responses are written,

$$\begin{aligned} \mathbf{X}_1(\mathbf{j}\omega) &= \mathbf{H}_{1,\mathbf{f}}(\mathbf{j}\omega) \mathbf{C}_f \\ \mathbf{X}_2(\mathbf{j}\omega) &= \mathbf{H}_{2,\mathbf{f}}(\mathbf{j}\omega) \mathbf{C}_f \\ &\vdots \\ \mathbf{X}_n(\mathbf{j}\omega) &= \mathbf{H}_{n,\mathbf{f}}(\mathbf{j}\omega) \mathbf{C}_f \end{aligned} \quad (10)$$

The reference response is represented by,

$$\mathbf{X}_r(\mathbf{j}\omega) = \mathbf{H}_{r,\mathbf{f}}(\mathbf{j}\omega) \mathbf{C}_f \quad (11)$$

where  $\mathbf{C}_f$  is the Fourier transform of the *flat spectrum* force.

Therefore, the row or column of the Response Spectra matrix corresponding to the reference response would be written,

$$\begin{aligned} \mathbf{G}_{1,r}(\mathbf{j}\omega) &= \mathbf{H}_{1,\mathbf{f}}(\mathbf{j}\omega) | \mathbf{C}_f | \mathbf{H}_{r,\mathbf{f}}(\mathbf{j}\omega)^* \\ \mathbf{G}_{2,r}(\mathbf{j}\omega) &= \mathbf{H}_{2,\mathbf{f}}(\mathbf{j}\omega) | \mathbf{C}_f | \mathbf{H}_{r,\mathbf{f}}(\mathbf{j}\omega)^* \\ &\vdots \\ \mathbf{G}_{n,r}(\mathbf{j}\omega) &= \mathbf{H}_{n,\mathbf{f}}(\mathbf{j}\omega) | \mathbf{C}_f | \mathbf{H}_{r,\mathbf{f}}(\mathbf{j}\omega)^* \end{aligned} \quad (12)$$

Each Response Spectrum in equation in (12) is equal to the product of a unique FRF multiplied by the flat force Auto Spectrum  $| \mathbf{C}_f |$  and the conjugate of the FRF between the force and the reference response.

Taking the *square root* of each Response Spectrum provides a row or column of data that is proportional to a row or column of FRFs, and is therefore suitable for curve fitting. A similar result is obtained when multiple (unknown) forces are assumed.

## Measurement Sets

The definition of a “shape” requires that all measured responses have correct magnitudes and phases relative to one another. In order to insure that a set of vibration measurements taken from two or more DOFs has the correct relative magnitudes and phases, two methods of measurement can be used [1],

1. Simultaneously acquire all responses together.
2. Simultaneously acquire some of the roving responses and a reference (fixed) response together as a measurement set.

An entire test then, consists of acquiring two or more measurement sets, with different roving responses and the same reference response in each measurement set. For large tests, where mode shapes with a large number for DOFs are desired, operating data is usually taken in multiple measurement sets.

### Force Level Changes

Force levels can change during the acquisition of multiple measurement sets of data. Therefore, to obtain valid shape data from multiple measurement sets where the force levels may have changed, the Response Spectrum magnitudes must be re-scaled.

One way to do this is to calculate an *average* of all of the reference Auto Spectra from the multiple measurement sets. Then, the magnitude of each Response Spectrum in a measurement set is re-scaled using the ratio of the average reference level to the reference level of the measurement set.

### Rational Fraction Polynomial Method Revisited

The Rational Fraction Polynomial (RFP) curve fitting method [6] was first implemented in a commercial FFT-based EMA system (the Hewlett Packard 5423A Structural Dynamics Analyzer), in the late 1970's. It has also been used in several other modal analysis packages including the SMS Star Modal and Vibrant Technology ME'scope software.

Rational Fraction Form

$$\mathbf{H}(\omega) = \frac{\sum_{k=0}^{2m-1} \mathbf{a}_k s^k}{\sum_{k=0}^{2m} \mathbf{b}_k s^k} \Big|_{s=j\omega} \quad (13)$$

Partial Fraction Form

$$\mathbf{H}(\omega) = \sum_{k=1}^m \left[ \frac{\mathbf{r}_k}{s - \mathbf{p}_k} + \frac{\mathbf{r}_k^*}{s - \mathbf{p}_k^*} \right] \Big|_{s=j\omega} \quad (14)$$

Figure 6. FRF Curve Fitting Models.

The RFP method uses the rational fraction polynomial instead of the partial fraction form of the FRF as its curve fitting model. These two models are shown in Figure 6. The RFP method solves a set of linear equations for the unknown numerator and denominator polynomial coefficients. Poles and residues are found by numerical root solving and partial fraction expansion, as shown in Figure 7.

Since the RFP method curve fits the FRF data directly, it can be used in small frequency bands to estimate the parameters of a small number of modes at a time. This makes it easier to use since the number of modal parameters obtained from a curve fitting operation is relatively small.

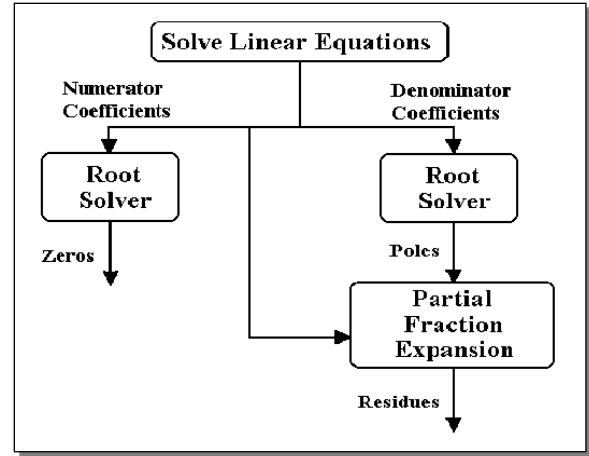


Figure 7. RFP Solution Process.

### Out-Of-Band Effects

In order to perform curve fitting in small frequency bands, any curve fitter must have a way to compensate for the effects of other modes that lie outside of the curve fitting band. The RFP method uniquely accounts for the effects of out-of-band modes by using a *higher order numerator* polynomial than the order required to estimate the residues. After the partial fraction expansion, these extra numerator terms are discarded.

### Global Curve Fitting

Orthogonal rather than ordinary polynomials are used to improve the numerical stability of the RFP method, but they also *uncouple* the numerator and denominator coefficient solution equations.

This allows the curve fitting problem to be divided into two steps. The denominator polynomial coefficients are estimated by a first curve fitting step, and hence the poles (modal frequency and damping) are estimated first. Then, the residues are estimated by a second curve fitting step.

Furthermore, the denominator equations can be reformulated so that data from two or more FRFs can be used to estimate the poles. This is called *global* curve fitting.

### Complex Exponential Revisited

This algorithm was first discovered by R. Prony in 1795 [9], and is therefore also been referred to as the Prony algorithm. It is used for curve fitting impulse response data using the complex exponential curve fitting model (6). Two of the most popular implementations of this method are the Time Domain Poly Reference method [8], and the Ibrahim Time Domain [9] method.

Two sets of linear solution equations are also created using the CE method. The first set, called the Toeplitz equations because of their special form, is solved for the coefficients of the characteristic polynomial (FRF denominator polynomial). The poles are then obtained as the roots of the characteristic polynomial. The second set of solution equations,

called the Van der Monde equations, is then solved for the residues.

The denominator polynomial equations can also be reformulated so that data from two or more IRFs can be used for curve fitting. This yields global estimates of the poles in the same manner as the RFP method.

The CE method works best with large frequency bands of FRF data (inverse FFT'd to provide the IRFs), and large numbers of modes at a time. Although it can be used on smaller frequency bands of data, it has no means of compensating for the effects of out-of-band modes like the RFP method. The only means available is to add extra *computational modes* to the curve fitting model, and discard them later from the results.

### Stability Diagram

Since the CE method must compensate for the effects of out-of-band modes by using extra computational modes, and since it is numerically stable even for a large numbers of modes, the best way to use it is with a stability diagram, as shown in Figure 8. A stability diagram is a plot of pole estimates for different curve fitting model sizes. A typical diagram may display solutions for one mode up to as many as 50 modes. The poles are typically plotted on top of Mode Indicator function. (Mode Indicators are discussed below.)

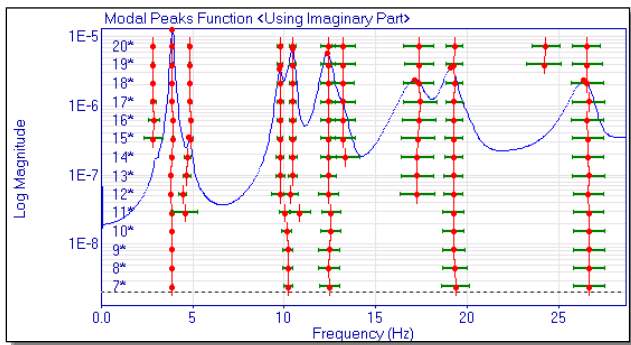


Figure 8. Stability Diagram.

A stability diagram has two advantages;

1. It helps the user determine how many modes are really contained in a frequency band.
2. By displaying a stable pole estimate for several model sizes, it confirms that the estimate is correct.

### Curve Fitting Steps

In general, curve fitting requires three steps;

1. Determine how many modes are represented in the data.
2. Estimate a pole for each mode.
3. Estimate a residue for mode.

A row or column of residues from the residue matrix corresponding to the same row or column of the FRF, IRF, or Response Spectrum matrix, is then saved as the mode shape.

### Mode Indicators

Mode indicator functions are used to help determine how many modes are represented in a set of experimental data. The number of modes is required in order to specify the curve fitting model size. Both the FRF curve fitting model (14) and the IRF curve model (6) involve the same summation over the number of modes ( $m$ ). Therefore,  $m$  must be determined before using these models.

### Modal Peaks Function

Since resonances are manifested by peaks in FRF or Response Spectrum data, the most straightforward way to find the number of modes is to count resonance peaks. Since a single measurement may not contain peaks for all of the modes, a Modal Peaks Function can be calculated by summing together squared values of all of the measurements in a data set. Figure 8 shows a Modal Peaks Function as part of the Stability Diagram.

### CMIF

The Complex Mode Indicator Function not only indicates model peaks, but it can also indicate closely coupled modes (two or more modes represented by a single peak) or repeated roots (two or more modes at the same frequency) [11]. If multiple references of data are used, then closely coupled modes or repeated roots can be indicated. Figure 9 shows a typical set of CMIF curves.

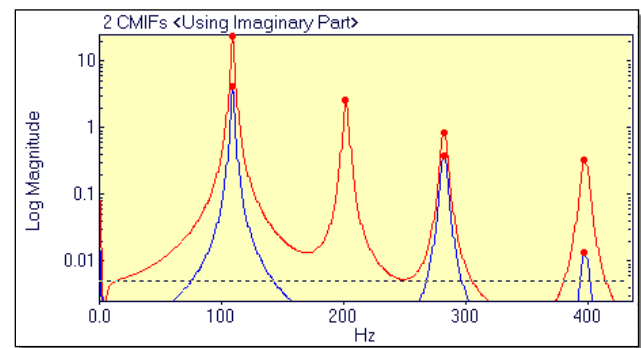


Figure 9. CMIF Indicating Three Repeated Roots.

### MMIF

The Multivariate Mode Indicator Function can also indicate closely coupled modes or repeated roots [12]. Figure 10 shows a typical set of MMIF curves.

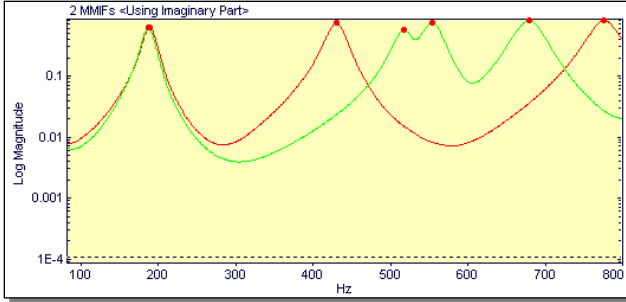


Figure 10. MMIF Showing Closely Coupled Modes at 200 Hz.

### Experimental Results

The RFP and Complex Exponential curve fitting methods will be applied to three different sets of modal test data. These three sets of multiple-channel time domain vibration data were taken from the Z24 highway bridge in Switzerland [13]. Each test was performed under different test conditions.

**Case 1: A two shaker test**, which provided acceleration response & excitation force time waveforms in nine measurement sets. The shakers were driven by uncorrelated random signals with non-zero spectrum values from 3 to 30 Hz.

**Case 2: An impact test**, which provided acceleration response time waveforms, including three reference (fixed) responses, in nine measurement sets. The impact force was provided by a 100 kg. drop weight impactor, but the *force was not measured*.

**Case 3: An ambient test**, which provided acceleration response time waveforms, including three reference (fixed) responses, in nine measurement sets. Excitation was provided by traffic on an adjacent bridge.

Two excitation forces were used in Case 1, so FRFs were calculated between all response DOFs and the two DOFs where the shakers were attached. Since no forces were measured in Cases 2 & 3, Response Spectra could be calculated for these two cases.

Ideally, all of the tests should yield the same modal parameters. In Case 1, since the bridge was excited with shakers driven by broad-band random signals, we would expect all of the modes in the 3 to 30 Hz frequency range to be excited. In Cases 2 & 3, the bandwidth of excitation is unknown.

### Case 1: Multi-Shaker Test

The data acquired for test Case 1 consisted of **117** time waveforms in nine measurement sets. Each time waveform consisted of 65536 samples of uniformly sampled data with a 0.01 second time increment between samples (or a 100 Hz sampling rate), giving a total time length of 655.35 seconds.

Each measurement set was processed using spectrum averaging, with a 2048 sample spectrum size, 20 spectral averages, and a Hanning window applied to reduce leakage [5]. The spectrum size and number of averages required overlap

processing percentage of 21%, meaning that about 1/5th of the samples from each sampling window (samples used per spectrum average) were used in the succeeding sampling window.

A total of 150 FRFs were calculated; 2 columns of an FRF matrix with 75 unique response DOFs and 2 reference shaker DOFs. A typical FRF is shown in Figure 11.

### Case 2: Impact Test

The data acquired for test Case 2 consisted of 126 time waveforms in nine measurement sets. Each time waveform consisted of 8192 samples of uniformly sampled data with a 0.01 second time increment between samples, giving a total time length of 81.92 seconds.

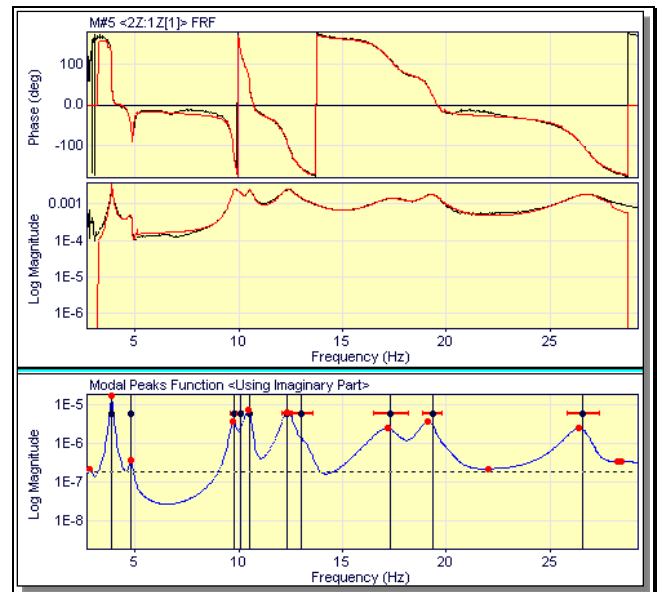


Figure 11. FRF and Curve Fit Overlaid.

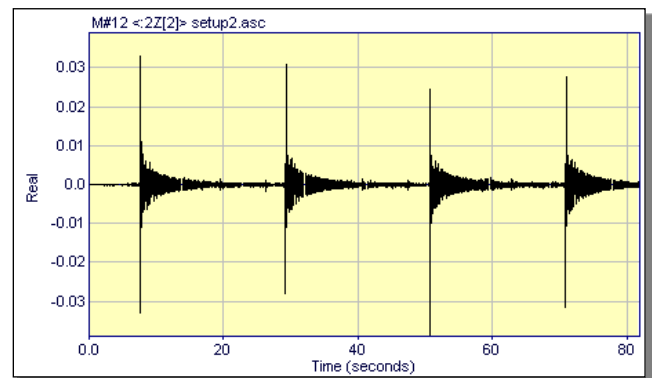


Figure 12. Typical Impact Time Waveform.

A typical time waveform is shown in Figure 12. Notice that the bridge was impacted and allowed to “ring down” 4 times over the 81 second acquisition period. Each measurement set was processed using spectrum averaging, with a 900

sample spectrum size and a trigger to begin each sampling window at the start of an impulse response. Since each signal contained 4 impulse responses, 4 spectral estimates were averaged together to form the Response Spectrum measurements.

A total of 215 Response Spectra were calculated; 3 columns of a Response Spectrum matrix with 75 unique response DOFs and 3 reference DOFs. A typical Response spectrum is shown in Figure 13.

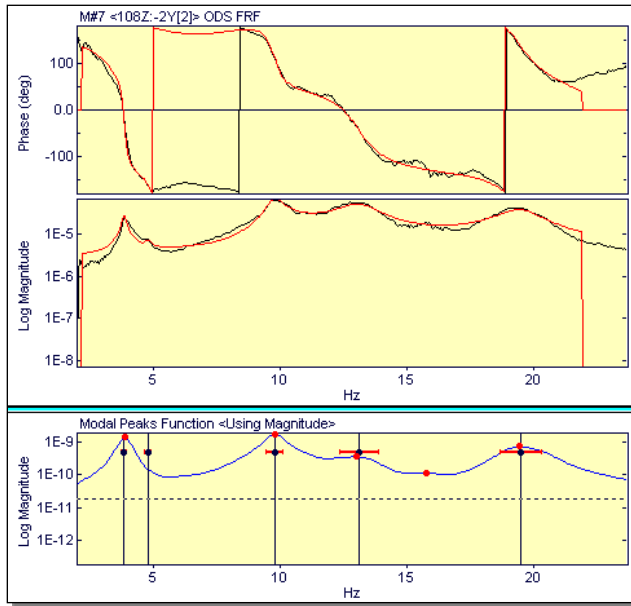


Figure 13. Impact Response Spectrum and Curve Fit Overlaid.

### Case 3: Ambient Test

The data acquired for test Case 3 consisted of 126 time waveforms in nine different measurement sets. Each time waveform consisted of 65536 samples of uniformly sampled data with a 0.01 second time increment between samples, giving a total time length of 655.35 seconds. A typical time waveform is shown in Figure 14.

Each measurement set was processed using spectrum averaging, with a 2048 sample spectrum size, 50 spectral averages, and a Hanning window to reduce leakage. The spectrum size and number of averages caused an overlap processing percentage of 69%.

A total of 215 Response Spectra were calculated; 3 columns of a Response Spectrum matrix with 75 unique response DOFs and 3 reference DOFs. A typical Response Spectrum is shown in Figure 15.

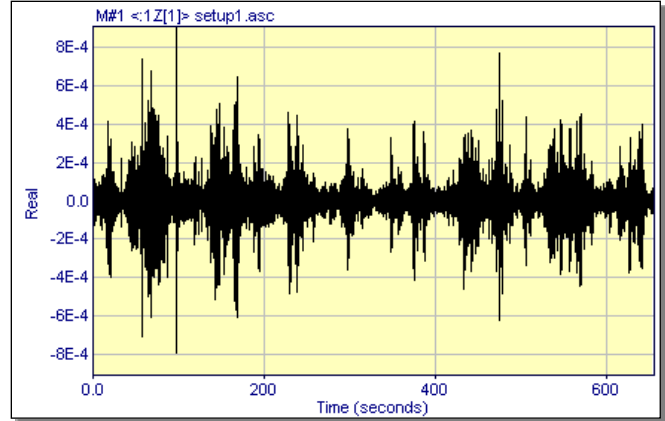


Figure 14. Typical Ambient Time Waveform.

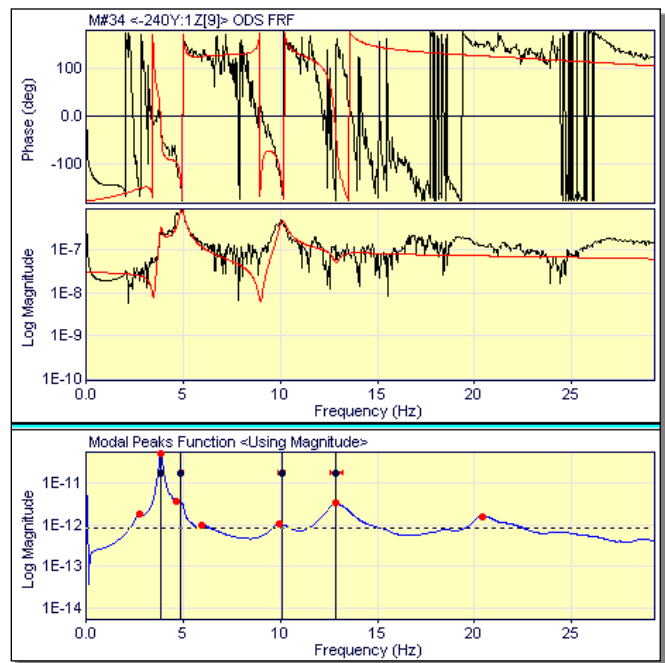


Figure 15. Ambient Response Spectrum and Curve Fit Overlaid.

### FRF Curve Fitting

The FRFs were curve fit using both the RFP and CE methods, and those modal parameters were used for comparisons with the Impact and Ambient curve fitting results. A typical FRF curve fit is shown in Figure 11.

### Modal Frequencies and Damping

Table 1 contains a comparison of the modal frequency and damping estimates obtained by the two curve fitting methods.

### Mode Shapes

Table 2 contains the Modal Assurance Criterion (MAC) values between the mode shape estimates from the two

curve fitting methods. *MAC values above 0.9 indicate that two shapes are nearly alike.*

MAC values are listed for shapes between the two references for each method, and between the *best* shape estimates of the two methods. The *best* shape was chosen as the one with the largest strength (highest average magnitude) between the two references.

The MAC values between references indicate that both references did not provide the same mode shape for all modes. Low MAC values between the methods indicate that even the best mode shape estimates of both methods didn't match for some modes.

Mode	Frequency (Hz)		Damping (Hz)	
	RFP	CE	RFP	CE
1	3.88	3.87	0.029	0.028
2	4.82	4.82	0.079	0.089
3	9.77	9.78	0.161	0.157
4	10.5	10.5	0.151	0.192
5	12.3	12.4	0.245	0.389
6	13.0	13.2	0.516	0.637
7	17.3	17.3	0.855	0.924
8	19.3	19.3	0.490	0.459
9	26.6	26.6	0.785	0.818

Table 1. FRF Modal Frequencies and Damping.

Mode	RFP (Between References)	CE (Between References)	RFP & CE
1	1.00	1.00	1.00
2	0.89	0.97	0.91
3	0.94	0.99	0.99
4	0.99	0.97	0.99
5	0.99	0.06	0.01
6	0.74	0.10	0.11
7	0.65	0.30	0.96
8	0.59	0.17	0.98
9	1.00	0.92	0.98

Table 2. FRF Mode Shape MAC Values.

Each of the three references of impact Response Spectrum data were curve fit using both the RFP and CE methods. Figure 13 shows at typical curve fit of an impact Response Spectrum.

Table 3 compares frequency and damping estimates from curve fitting the three references of Impact data with the FRF modes. Only the results of the RFP method are shown, but the CE results are similar.

Mode	Frequency (Hz)			
	RFP	Ref 1	Ref 2	Ref 3
1	3.88	3.85	3.84	3.86
2	4.82	4.91	4.80	4.79
3	9.77	9.76	9.76	9.78
6	13.0	13.4	13.2	13.1
8	19.3	19.3	19.4	19.5

Table 3A. Impact Modal Frequencies.

Mode	Damping (Hz)			
	RFP	Ref 1	Ref 2	Ref 3
1	0.029	0.049	0.073	0.060
2	0.079	0.076	0.091	0.089
3	0.161	0.230	0.297	0.286
6	0.516	1.06	0.580	0.730
8	0.490	0.638	0.562	0.770

Table 3B. Impact Modal Damping.

Table 4 contains the mode shape MAC values between mode shapes for each of the three impact references and the FRF mode shapes.

Mode	FRF & Ref 1	FRF & Ref 2	FRF & Ref 3
1	0.97	0.98	0.99
2	0.40	0.26	0.97
3	0.90	0.96	0.96
6	0.01	0.24	0.15
8	0.90	0.93	0.94

Table 4 Impact Mode Shape MAC Values.

### Ambient Curve Fitting

Each of the three references of ambient Response Spectrum data were curve fit using both the RFP and CE methods. Figure 15 shows at typical curve fit of an Ambient Response spectrum.

Table 5 compares frequency and damping estimates from curve fitting the three references of Ambient data with the FRF modes. Again, only the results of the RFP method are shown but the CE results are similar.

Table 6 contains the mode shape MAC values between mode shapes for each of the three impact references and the FRF mode shapes.

Mode	Frequency (Hz)			
	RFP	Ref 1	Ref 2	Ref 3
1	3.88	3.85	3.86	3.85
2	4.82	4.88	4.94	4.92
3	9.77	10.1	-----	9.91
6	13.0	12.9	-----	-----

Table 5A. Ambient Modal Frequencies.

Mode	Damping (Hz)			
	RFP	Ref 1	Ref 2	Ref 3
1	0.029	0.049	0.049	0.047
2	0.079	0.092	0.059	0.066
3	0.161	0.153	-----	0.123
6	0.516	0.302	-----	-----

Table 5B. Ambient Modal Damping.

Mode	FRF & Ref 1	FRF & Ref 2	FRF & Ref 3
1	0.99	0.98	0.93
2	0.53	0.85	0.81
3	0.38	-----	0.75
6	0.57	-----	-----

Table 6 Ambient Mode Shape MAC Values.

## CONCLUSIONS

Modal parameter estimation was applied to experimental data that was taken during three separate tests of a concrete and steel highway bridge.

The first test was performed using two shakers driven by random excitation signals to excite the bridge. FRFs were calculated during post-processing using digital signal processing methods that are commonly available in many multi-channel FFT analyzers. This case represents a traditional modal test.

The second and third test cases are representative of operating data tests. In tests similar to these two cases, it is not possible to control or measure the forces exciting a structure. Yet these results show that meaningful modal parameter estimates can still be obtained from *response only* (or *operating*) data.

Mode shapes of the 4 modes common to all tests are shown in Figure 16. The first bending mode at 2.8 Hz was easily excited by all three tests, and all of the curve fitting results agree closely with one another. The second modes, a transverse torsional mode of the bridge, was not excited as well in the ambient test, so its mode shape estimates have significant errors, i.e. MAC values less than 0.90.

As expected, Case 1 yielded the best results. Whenever FRFs can be measured under controlled conditions where

the excitation forces are measured, the modal parameter estimates are usually the most accurate.

It is clear from the measurements that fewer modes were excited by impacting (Case 2) than with the two shakers, and even fewer modes were excited by ambient excitation (Case 3). Nevertheless, the results clearly show that the first two modes (3.8 & 4.8 Hz) could be estimated with acceptable accuracy by curve fitting the operating data from cases 2 and 3..

All of the post-processing and graphics presented in this paper were done with the ME'scopeVES™ software from Vibrant Technology, Inc.

## References

- [1] Vold, H., Schwarz, B. & Richardson, M., Display Operating Deflection Shapes from Non-Stationary Data, Sound & Vibration Magazine June 2000.
- [2] Richardson, M., Is It A Mode Shape Or An Operating Deflection Shape?, Sound and Vibration Magazine, February 1997.
- [3] Pickrel, C. R., Airplane Ground Vibration Testing – Nominal Modal Model Correlation, Sound and Vibration Magazine, November, 2002.
- [4] Batel, M. Operational Modal Analysis – Another Way of Doing Modal Testing, Sound and Vibration Magazine, August 2002.
- [5] Richardson, M., Structural Dynamics Measurements, Structural Dynamics @ 2000: Current Status and Future Directions, Research Studies Press, Ltd. Baldock, Hertfordshire, England December, 2000, p-341.
- [6] Formenti, D. & Richardson, M. Parameter Estimation From Frequency Response Measurements Using Rational Fraction Polynomials (Twenty Years Of Progress), Proceedings of International Modal Analysis Conference XX, February 4-7, 2002 Los Angeles, CA.
- [7] Brown, D. & Allemang, R. Multiple Input Experimental Modal Analysis, Fall Technical Meeting, Society of Experimental Stress Analysis, Salt lake City, UT, November, 1983.
- [8] Vold, H., Kundrat, J., Rocklin, G. A Multi-Input Modal Estimation Algorithm for Mini-Computers, S.A.E. paper No. 820194, 1982.
- [9] Ibrahim, S., Mikulcik, E. A Method for the Direct Identification of Vibration Parameters from the Free Response, Shock and Vibration Bulletin, Vol 47, Part 4, 1977.
- [10] Improvements in the Complex Exponential Computational Algorithm, Office of Naval Research, Washington, DC., prepared by Texas Instruments, Dallas, TX., March, 1970.

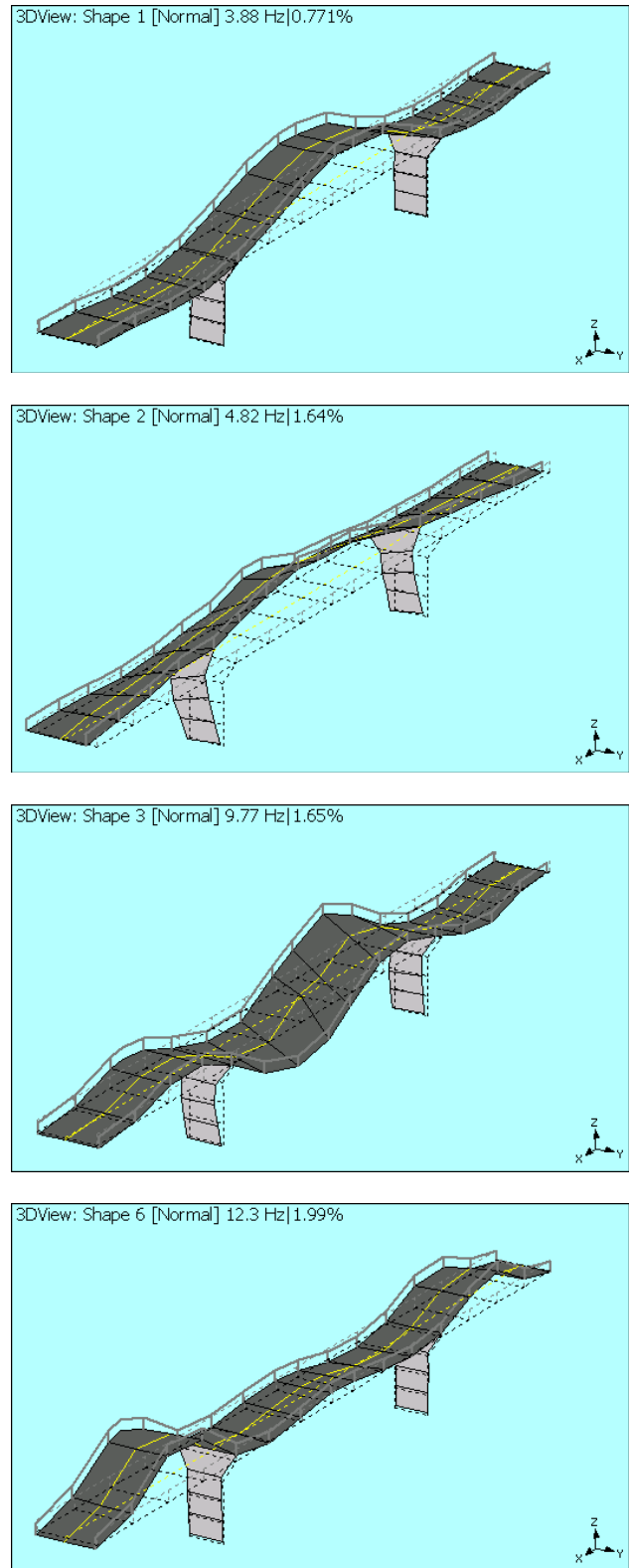


Figure 16. Mode Shape Estimates of the Bridge.

[11] Shih, C., Tsuei, Y., Allemang, R., Brown, D., Complex Mode Indication Function and its Applications to Spatial Domain Parameter Estimation, Proceedings of International Modal Analysis Conference VII, January, 1989.

[12] Williams, R., Crowley, J., Vold, H., The Multivariate Mode Indicator Function in Modal Analysis, Proceedings of International Modal Analysis Conference III, January, 1985.

[13] Peeters, B., Ventura, C., Comparative Study of Modal Analysis Techniques for Bridge Dynamic Characteristics, submitted to Mechanical Systems and Signal Processing, 2001.